Elastic constants of body-centered-cubic cobalt films

S. Subramanian and R. Sooryakumar
Department of Physics, The Ohio State University, Columbus, Ohio 43210

G. A. Prinz, B. T. Jonker, and Y. U. Idzerda
Naval Research Laboratory, Washington, D.C. 20375

(Received 9 April 1993; revised manuscript received 13 January 1994)

The wave-vector and directional dependence of the Rayleigh elastic wave localized in epitaxial films of bcc cobalt are measured by Brillouin scattering. The Rayleigh velocities are well described by elastic continuum theory and yield values for the C_{11} and C_{44} elastic constants that are reduced to about 65% of the corresponding values in the thermodynamically stable hcp configuration. While the reduction in C_{11} in these supported films (several hundred angstroms thick) is consistent with recent calculations for bulk bcc cobalt, the C_{44} and C_{12} values we have derived are significantly smaller than those predicted by the theory. The C_{ij}'s determined independently from the Rayleigh wave dispersion along distinct crystallographic directions in films of different orientations agree well.

I. INTRODUCTION

An understanding of the delicate interplay between configurational and magnetic energies in itinerant ferromagnets currently presents a critical test of first-principle calculational techniques to determine the electronic structure of metals. This is especially challenging since the energy difference between two distinct crystal structures may be comparable to the small energy differences associated with magnetic effects. Cobalt, which can be stabilized as thin supported epiaxial films in the naturally occurring hexagonal-closed-packed phase as well as face- and body-centered-cubic configurations,[1-3] offers an excellent model system to test these calculations. bcc cobalt also has the distinction of being one of the most strongly correlated $3d$ transition metals. Correlations will play an important role in establishing the properties of the different phases of cobalt, since the relative strength of the electron-electron interaction determines the competition between delocalization due to band formation and localization due to Coulomb coupling between electrons. Friedel and Sayers[4] have discussed the effects of correlations on the lattice constant and bulk moduli B for $3d$ elements, and show that for elements near the middle of the series electron-electron interactions strongly influence these properties. They also note that while nonmagnetic midrow $3d$ elements should show substantial elastic softening compared with the zero correlation values, the softening of B should be further enhanced when these elements become magnetic. A determination of the elastic properties of the different phases of cobalt will hence be valuable toward experimentally establishing the role of correlations on the bulk moduli of transition metals.

Studies on different phases of Co have also focused on better understanding magnetic anisotropy, e.g., the tendency of the easy axis of magnetization to display thickness and orientational dependence in laminar and superlattice geometries.[5-10] Phenomenological models considering contributions from the magnetocrystalline, magnetoelastic, and demagnetization anisotropy energies have been utilized to describe the latter.[5-8] The importance of magnetoelastic contributions to the magnetic anisotropy in epitaxial Co structures has been recognized in several publications.[6,8,11] The elastic constants hence not only provide direct insight into the microscopic nature of bonding, but also place important constraints on the reliability of calculations of *magnetic* properties.

In this paper we report on measurements of the three independent elastic constants of several relatively thick single-crystalline Co films stabilized in the bcc phase. The elastic properties of this Co phase are determined through the Rayleigh phonon of the coupled layer (Co)–substrate (GaAs) system by Brillouin light scattering. The C_{ij}'s determined independently from a study of the Rayleigh wave propagation along special crystallographic directions on film surfaces of different orientations are found to agree well. In agreement with recent local-spin-density approximation calculations for the elastic properties of bulk bcc cobalt by Liu and Singh,[12] the measured C_{11} constant is reduced by about 65% of its corresponding value in the hcp phase. However, the C_{12} and C_{44} constants we have experimentally determined are significantly lower than those calculated[12] for the bulk.

II. EXPERIMENT

Four bcc Co films were grown on GaAs substrates by molecular-beam epitaxiay (MBE) techniques, as described elsewhere.[3] Two of the metal films were oriented with the (110) plane parallel to the film surface, and were 357 and 202 Å thick. The other two films, 106 and 125 Å thick, were grown on the (001) face of GaAs and thus oriented with the (001) plane parallel to the substrate. The epilayer thickness (h) has been measured to an accuracy of about two monolayers.

Each film was confirmed to be of bcc phase through x-ray diffraction. The bcc structure of the two thickest Co films (357 and 202 Å) has also been confirmed by conversion electron extended x-ray-absorption fine structure

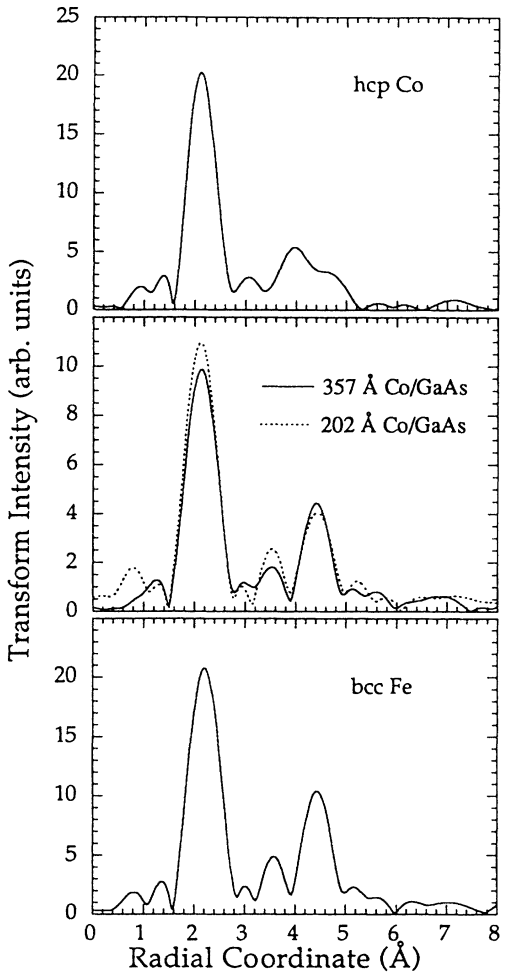

FIG. 1. Radial distribution function of the Fourier-transformed extended x-ray-absorption fine-structure spectra for hcp Co, the 357- and 202-Å films deposited on GaAs and bcc Fe. Note that the transforms show conclusively that the two Co films have nearly identical spectra, and are very similar to the bcc spectra of Fe but very different from the hcp Co spectra.

(EXAFS).[13] In Fig. 1 we present the radial distribution function of the films of Co deposited on GaAs, and bcc Fe. Inspection of the transforms shows conclusively that the two Co films have nearly identical spectra, and are very similar to the bcc Fe spectra but very different from the hcp Co spectra. [The Fourier-transformed EXAFS spectra for fcc Co is similar to the spectra of hcp Co (Ref. 13).] The strong similarity between the spectra for the bcc Fe and the two Co films confirms that both films are bcc structures. The radial coordinate of Fig. 1 does not include phase-shift correction factors, and therefore does not represent the actual internuclear spacings for these materials. Additional details of the EXAFS measurement process and analysis procedures can be found in Ref. 13, where the bcc structure was first demonstrated.

The Brillouin scattering measurements were performed at room temperature in a backscattering geometry with a six-pass tandem Fabry-Perot interferometer using the 5145-Å Ar-ion or 6471-Å Kr-ion laser line. Different sets of interferometer plates suitably coated for use with each of the two exciting laser lines were utilized. The polarization of the incident beam was in the sagittal plane (i.e., p polarized) and the scattering was recorded in a $p \rightarrow p$ geometry when phonon features had to be isolated from spin-wave contributions. Magnons were separated by analyzing s-polarized radiation normal to the saggital plane. The spectra were measured with an incident laser power of 120–150 mW with a sampling time of about 3 h per spectrum. The in-plane wave-vector component of the Brillouin modes, q, in each film was measured by varying the angle of incidence θ_i between 30° and 70°. The angle was measured to an accuracy of $\pm 0.1°$. For the smaller angles of incidence it was necessary to reduce the aperture from $f/1.4$ to $f/3.5$ to compensate for increased broadening.

III. EXPERIMENTAL RESULTS

Figures 2 and 3 show typical Brillouin spectra from the two thicker films. Figures 2(a) and 2(b) were recorded at

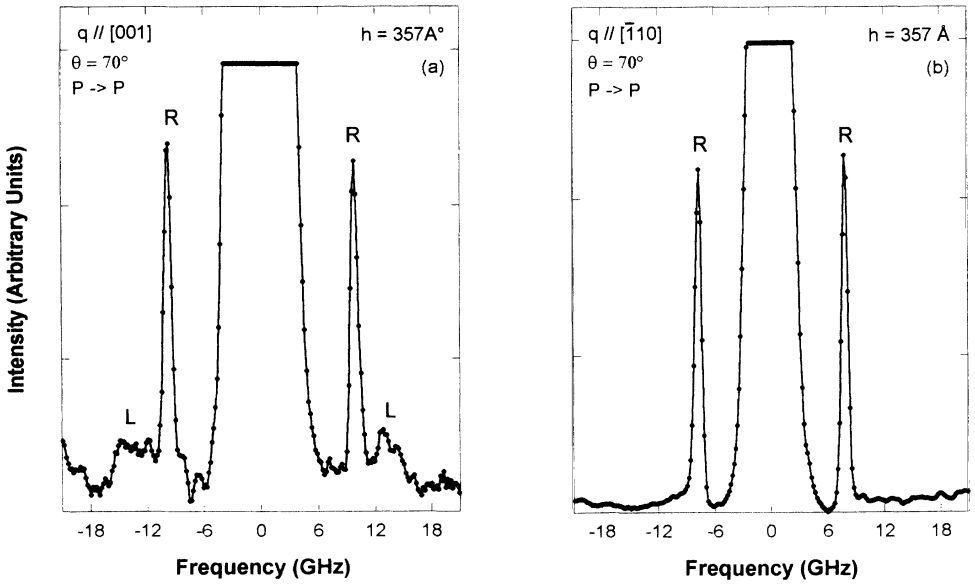

FIG. 2. Brillouin spectra from 357-Å-thick bcc cobalt film in $p \rightarrow p$ scattering geometry, and an angle of incidence of 70°. R identifies the Rayleigh mode, and L the Lamb wave continuum. (a) In-plane wave-vector transfer parallel to [001]. (b) In-plane wave-vector transfer parallel to [$\bar{1}$10].

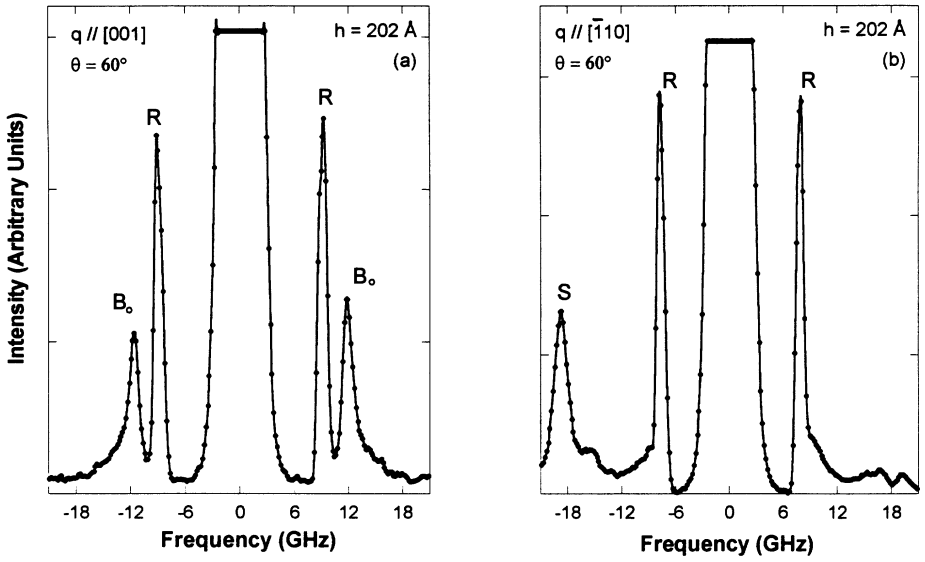

FIG. 3. Brillouin spectra from 202-Å-thick bcc cobalt film at an angle of incidence of 60°. The scattered radiation was not analyzed. R identifies the Rayleigh mode, while S and B_0 are surfacelike and bulklike magnons. (a) In-plane wave-vector transfer parallel to [001]. (b) In-plane wave-vector transfer parallel to [$\bar{1}$10].

an angle of incidence of 70° with **q** along [001] and [$\bar{1}$10] on the 357-Å film. Similar phonon features were observed in the 106- and 125-Å films. The Rayleigh mode R is identified, while the shoulder labeled L arises from scattering by Lamb waves. Magnon scattering, which includes the surface and discrete exchange-dominated bulk spin waves, has been suppressed in these spectra through polarization selection. Figure 3 shows data from the 202-Å film measured at $\theta_i = 60°$ and, in this case, spin-wave features are retained by not analyzing the scattered beam. Strong Rayleigh peaks R are observed in addition to surfacelike (S) and bulklike (B_0) magnons. The magnetic nature of the latter excitations was confirmed through polarized ($p \rightarrow s$) scattering, and their response to a magnetic field.[14] Within the free spectral range shown in Fig. 3 the only magnetic excitation for wave-vector transfer along [001] are bulklike modes B_0, with no discernible intensity asymmetry for Stokes/anti-Stokes scattering. However, when **q** was directed along [$\bar{1}$10], a surfacelike magnetic mode S, with characteristic appearance on either the Stokes or anti-Stokes spectrum, is seen in Fig. 3(b). This directional-dependent magnon scattering is a manifestation of the magnetic anisotropy, where the surface mode is unstable against decay into bulklike modes for propagation along the easy axis of magnetization.[15]

The phase velocities V_s of the Rayleigh mode R were measured for propagation along the [001] and [$\bar{1}$10] directions in (110)-oriented films, while velocities along [100] and [110] were determined from the (001) samples. In all cases V_s was obtained by dividing the measured Brillouin frequency by q ($=2K_i \sin\theta_i$, where K_i is the

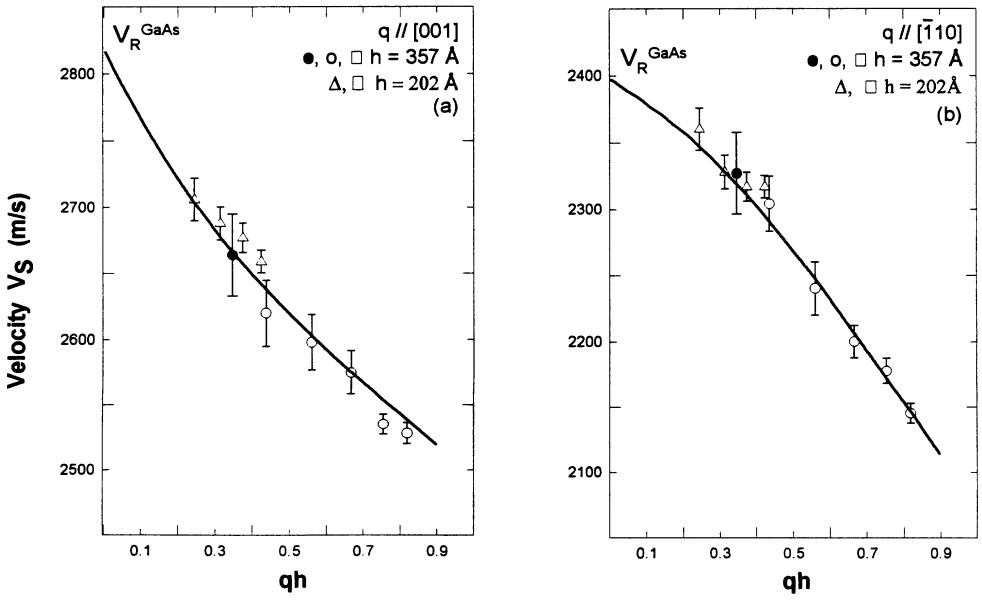

FIG. 4. The measured (○, ●, and △) and calculated (solid line) dispersion curves for the principal mode Rayleigh mode for 357- and 202-Å-thick bcc cobalt films on (110) GaAs. The two panels refer to propagation directions along [001] and [$\bar{1}$10]. Data represented by ○ and △ were taken with 5145-Å radiation, while ● was taken at 6471 Å.

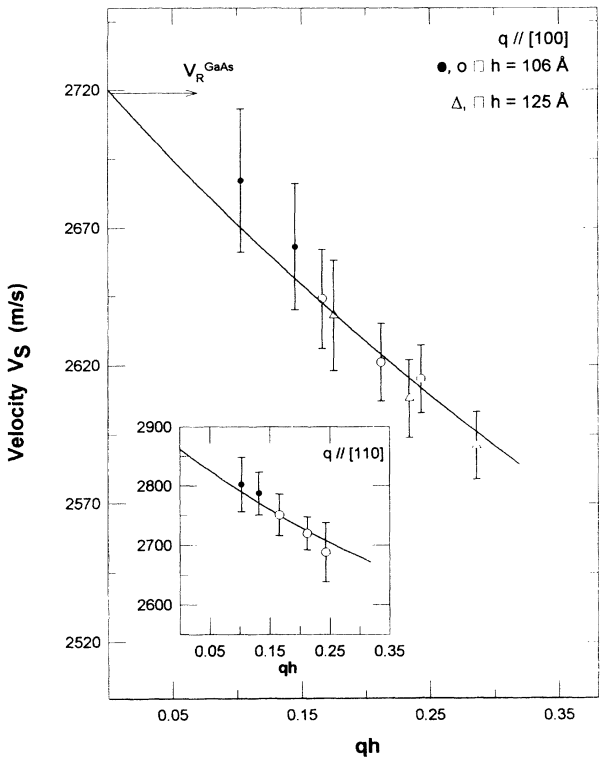

FIG. 5. The measured (○, ●, and △) and calculated (solid line) dispersion curves for the principal mode Rayleigh mode for 106- and 125-Å-thick bcc cobalt films on (001) GaAs. Inset shows measured Rayleigh velocities along [110] for the 106-Å film. The solid line is the calculated velocity utilizing elastic constants as derived from data for in-plane wave-vector transfer parallel to [001]. ● refers to data acquired with 6471 Å from the 106-Å epilayer. The other data were recorded at 5145 Å.

wave vector of the incident beam). Results for the measured dispersion of V_s as a function of qh are summarized in Figs. 4 and 5. The data associated with the 6471-Å exciting laser line is indicated by the filled circle symbol; the other symbols indicate data acquired with 5145-Å radiation. It can be seen that the measured Rayleigh velocities are in good agreement with the calculations described below and shown as solid lines in Figs. 4 and 5.

IV. DISCUSSION

For body-centered-cubic cobalt on (110) GaAs, the acoustic modes with **q** along [$\bar{1}$10] and [001] consist of decoupled partial waves with displacements polarized in the sagittal plane and normal to this plane.[16] The principal mode in the former case is the Rayleigh wave. Solutions for the corresponding higher-order modes (Sezawa waves) exist only for cobalt film thicknesses greater than those utilized in this study. The modes with displacements perpendicular to the sagittal plane are Love modes.[16] Such excitations are not observed in our measurements because of the negligible associated surface ripple and weakness of elasto-optic scattering from metal surfaces. The velocities of the Rayleigh waves have been calculated by taking into account the mechanical boundary conditions at the film interfaces—the vanishing of stress components normal to the layer at the free surface, and continuity of the displacement components at the interface.

Based on the elastic continuum theory[16,17] for a thin film on a cubic substrate, we calculate the best fits to the measured velocity dispersion. The elastic constants of bulk hcp Co (Ref. 18) were used as initial inputs to the fitting procedure for each heterostructure. We take the bulk elastic parameters for the GaAs substrate to be unmodified as a result of the epitaxial growth. The density of the epilayers was estimated (8.83×10^3 kg/m^3) from the measured[3] lattice constant of the 357-Å-thick bcc cobalt film; this density is very close to that of bulk hcp Co. The calculated dispersion for Rayleigh mode propagation along [001] and [$\bar{1}$10] in the two (110)-oriented films are shown as solid lines in Figs. 4(a) and 4(b). The fits to the data for the two propagation directions were obtained with a single set of C_{11}, C_{44}, and C_{12} constants. We observe that while the fit provides an overall good description, the data for the same qh ($=0.43$) from the two films lie slightly outside their error margins. This feature could reflect some differences between the elastic constants of the two films, although such differences will be within the quoted error for the C_{ij}'s. As discussed below strain effects may give rise to these small modifications. The second column in Table I summarizes the resulting best-fit elastic constants for these two films. The C_{11} (193 GPa) and C_{44} (48 GPa) values for the (110) bcc cobalt films are considerably smaller (reductions of 40% and 35%, respectively) than those already reported for the bulk hcp phase.[18] The C_{12} (163 GPa) constant is not changed significantly from the hcp value.

The elastic constants for the 106- and 125-Å epilayers that are (001) oriented were similarly obtained by fitting the corresponding V_s for [100] propagation. The use of two different excitation wavelengths enabled a wider range of qh to be accessed in these films of limited thickness. The results of the fits are shown as solid lines in

TABLE I. Measured elastic constants for bcc, Co, in GPa, derived from fits to the Rayleigh wave dispersion data. Calculated values for the C_{ij}'s in the bcc phase are quoted from Ref. 12. The values for the hcp and fcc phases are included for comparison.

C_{ij}	bcc Co[a] measured	bcc Co[b] measured	bcc Co[c] calculated	hcp Co[d] measured	fcc Co[e]
C_{11}	193±10	212±21	205	307.0	242
C_{12}	170±12	165±17	278	165	160
C_{44}	48 ±6	53±10	152	75.3	128

[a]This work—357- and 202-Å (110) films grown on GaAs.
[b]This work—106- and 125-Å (001) films grown on GaAs.
[c]Reference 12.
[d]O. L. Anderson, *Physical Acoustics* (Academic, New York, 1965), Vol. 3-B, Chap. 2.
[e]R. F. S. Hearmon, *Elastic, Piezoelectric and Related Constants of Crystals,* Landolt-Börnstein, New Series, Group III, Vol. 18 (Springer-Verlag, Berlin, 1984), Chap. S1.2, Table S3.

Fig. 5, and yielded the following values for the elastic constants: $C_{11}=212$ GPa, $C_{12}=165$ GPa, and $C_{44}=53$ GPa. The error margins on these values are slightly larger than those deduced for the (110) films discussed above and reflects, in part, the restrictions on the extent of qh. As seen from Table I, the elastic constants determined independently from the bcc Co films of different orientations are in good agreement with each other. As a further check of the consistency of the results, the Rayleigh wave dispersion along the [110] direction of the 106-Å (001) film was also determined. The inset to Fig. 5 illustrates these results. It shows excellent agreement with the measured Rayleigh velocities along the [110] direction for the 106-Å film, with the calculated V_s utilizing the C_{ij}'s determined from the dispersion for q parallel to [100] in these (001) epilayers.

In our evaluation of error margins for the calculated elastic constants, a threshold error T ($=\Sigma e_i$, where e_i is the error associated with a measured of V_s) was established for wave propagation along [001] and [110], and those values of C_{11}, C_{12}, and C_4 that satisfied $\Sigma[(V_{si}^{\text{expt}}-V_{si}^{\text{calc}})]<T$ simultaneously for propagation along both directions were considered acceptable. The errors e_i varied between 0.5 and 2%, with the largest contribution to e_i being derived from the measurement of the Brillouin shift. The uncertainties assigned to the elastic constants represent the spread in acceptable values of these constants as demanded by the threshold criteria. These error margins for C_{ij} can hence be viewed as a measure of the sensitivity of the Rayleigh velocity in the thin films to the corresponding elastic constants. Even though the Rayleigh wave is often most sensitive to C_{44}, in our case the error margins associated with the other elastic constants are comparable to that deduced for C_{44}. The reason for this most likely arises from the fact that C_{11} in these films is about four times larger than C_{44}.

In a recent calculation Liu and Singh[12] evaluated the elastic constants of *bulk* bcc cobalt, and the values for C_{44} and C_{12} are significantly higher than those reported here for supported epilayers. There is much closer agreement between the calculated and measured C_{11}. These calculated values are included in Table I, as are prior measured values for the elastic constants of the hcp and fcc phases of Co. It is noted in Ref. 12 that the calculated elastic constants, together with the minimal lattice mismatch between epilayer and GaAs substrate, are generally consistent with the epilayer, maintaining coherency to thicknesses of the order of tens of angstroms. Beyond this critical thickness the interfacial energy will be unable to stabilize the bcc phase. Given the reduced elastic constants for the bcc cobalt films measured in our experiments, it is conceivable that the interfacial energy remains dominant and thus continues to stabilize the bcc phase in our films beyond the critical thickness of about 50 Å.[19] In fact the homogeneous samples investigated in the present work are among the thickness bcc phase Co films produced.

What causes the reduction in the elastic constants while maintaining the bcc phase? At present we have no definitive answer. One possibility would be that our measurements probe surface phonons. However, these excitations decay well into the film, and thus bulk, rather than surface, elastic properties of the film are being probed. Reduction in elastic constants can arise from changes to the lattice parameters; the cubic lattice constant of 2.827 Å was measured for the 357-Å film, and is about 3% larger than the value predicted in Ref. 12. We believe this underestimate in the calculated a_0, while typical of local-spin-density approximations, would be inadequate to explain the dramatic reduction in C_{44} we have found. Strain effects can lead, through higher-order terms, to changes in the elastic constants and to a thickness dependence of the C_{ij}'s. The close lattice match between epilayer and substrate, which in fact aided in the choice of GaAs as a substrate, would argue for such effects being not significant. The small differences in the C_{ij}'s between the (110) and (001) layers may be due to differences in film quality associated with the growth of distinct film orientations.

Aside from extrinsic factors such as the growth rate, specific fabrication conditions, and structural defects, strong electron-electron correlations that characterize the bcc Co films could also influence the elastic properties in relation to the hcp phase. This connection between correlations and elastic stability in transition metals was first discussed by Friedel and Sayers.[4] The relative strength of the electron-electron interaction is governed by U/W, where U and W are the intra-atomic Coulomb energy and the bandwidth respectively. The bandwidth of metastable bcc cobalt is approximately 1.5 eV smaller than that of hcp Co,[20] so that U/W of bcc cobalt is $\sim$30% larger than that of the thermodynamically stable hcp modification. Correlations were shown[4] to reduce the bulk modulus B, the reduction being strongest near the middle of $3d$ series. From Table I we deduce that our measured value of B ($=[C_{11}+2C_{12}]/3=173$ GPa) for the bcc cobalt films is reduced by 10% from the hcp value.[18] Estimates based on Eq. (9) of Ref. 4 for the relative change between the bulk moduli in the hcp and bcc *bulk* phases of Co suggest that correlations would result in a $\sim$30% reduction in B. However, the fact that our Co epilayers are in registry with the substrate would tend to inhibit effects of correlations on the lattice expansion that would otherwise occur in the bulk phase. This constraint on the in-plane lattice parameters may be important in accounting for the degree of suppression in C_{11} and C_{44} we have determined. Careful considerations of the effects of extrinsic causes discussed above must, however, be systematically examined prior to identifying electron-electron correlations as an important source of the reduced C_{ij}'s we have determined for the bcc cobalt films.

V. SUMMARY

In summary, we have measured the elastic constants of several films of the bcc phase of Co by Brillouin light-scattering experiments. The measured Rayleigh phonon-dispersion curves of Co on GaAs are well described by elastic continuum theory. The C_{11} and C_{44} elastic constants in this case are reduced by almost 40 and 35% from their respective values in the thermo-

dynamically stable hcp phase. The C_{ij}'s determined independently from the Rayleigh wave dispersion along distinct crystallographic directions in films of different orientations agree well. Although the measured value of C_{11} is in agreement with recent linearized augmented-plane-wave calculations, the C_{44} and C_{12} values we have determined experimentally are significantly smaller than those predicted in Ref. 12. While some possible reasons for these differences between experiment and theory have been discussed, it would be valuable to have additional theoretical insight into the role of electron correlations on the elastic properties of this strongly correlated 3*d* metal.

ACKNOWLEDGMENTS

We thank A. Liu and D. Singh for making Ref. 12 available to us prior to publication. Several valuable discussions with J. Karanikas are also acknowledged. Work at OSU was supported by the National Science Foundation under Grant Nos. DMR90-0167 and 93-03568, and that at NRL by the Office of Naval Research.

[1]C. H. Lee, Hui He, and F. Lamelas *et al.*, Phys. Rev. Lett. **62**, 653 (1989).
[2]F. J. Lamelas, C. H. Lee, and Hui He *et al.*, Phys. Rev. B **40**, 5837 (1989).
[3]G. A. Prinz, Phys. Rev. Lett. **54**, 1051 (1985).
[4]J. Friedel and C. M. Sayers, J. Phys. (Paris) Lett. **38**, L263 (1977).
[5]F. J. A. den Broeder, D. Kuiper, A. P. van de Mosselaer, and W. Hoving, Phys. Rev. Lett. **60**, 2769 (1988).
[6]C. H. Lee, Hui He, and F. J. Lamelas *et al.*, Phys. Rev. B **42**, 1066 (1990).
[7]Brad. N. Engel, C. England, and R. A. Van Leeuwen *et al.*, J. Appl. Phys. **69**, 5643 (1991).
[8]Brad. N. Engel, C. England, and R. A. Van Leeuwen *et al.*, Phys. Rev. Lett. **67**, 1910 (1991).
[9]F. J. A. den Broeder, D. Kuiper, H. C. Donkersloot, and W. Hoving, Appl. Phys. A **49**, 507 (1989).
[10]C. H. Lee, R. F. C. Farrow, C. J. Liu, E. E. Marinero, and C. J. Chien, Phys. Rev. B **42**, 11 384 (1990).
[11]P. Bruno and J. P. Renard, Appl. Phys. A **49**, 499 (1989).
[12]A. L. Liu and D. J. Singh, Phys. Rev. B **47**, 8515 (1993).
[13]Y. U. Idzerda, W. T. Elam, B. T. Jonker, and G. A. Prinz, Phys. Rev. Lett. **62**, 2480 (1989).
[14]J. Karanikas, R. Sooryakumar, G. Prinz, and B. T. Jonker, J. Appl. Phys. **69**, 6120 (1991).
[15]S. Subramanian *et al.* (unpublished).
[16]G. W. Farnell and E. Adler, in *Physical Acoustics*, edited by W. Mason and R. N. Thurston (Academic, New York, 1972), Vol. IX.
[17]B. A. Auld, *Acoustic Fields and Waves in Solids* (Wiley, New York, 1973), Vols. 1 and 2.
[18]H. J. McSkimin, J. Appl. Phys. **26**, 406 (1955).
[19]P. C. Riedi, T. Dumalow, M. Rubenstein, G. A. Prinz, and S. B. Qadri, Phys. Rev. B **36**, 4595 (1987).
[20]D. J. Singh, Phys. Rev. B **45**, 2258 (1992).